MULTISCALE MECHANICAL CHARACTERIZATION OF BIOMIMETIC GELS FOR ARMY APPLICATIONS

Thomas F. Juliano, Paul Moy, Aaron M. Forster, Tusit Weerasooriya, and Mark R. VanLandingham*
U. S. Army Research Laboratory, Weapons & Materials Research Directorate
Aberdeen Proving Ground, MD, 21005

Peter L. Drzal
PPG Industries, Inc., 4325 Rosanna Drive, Allison Park, PA 15101

ABSTRACT

Ballistic gelatin often serves as a tissue surrogate for impact testing. Unfortunately, this material exhibits issues such as mechanical instability at room temperature and is difficult to structurally modify. A material system that is not as sensitive to these issues is styrene-isoprene triblock copolymer gels. In this work, two such copolymer gels were compared to ballistic gelatin via mechanical behavior evaluation using both macro-scale and micro-scale measurements. Both copolymer gels were found to have a greater degree of thermal stability than ballistic gelatin, and results based on mechanical evaluation show that the copolymer gels may be suitable as a replacement for ballistic gelatin.

1. INTRODUCTION

Understanding effects of blunt trauma injuries to thoracic organs is critical for the design of protective equipment used in the automotive, body armor, and sports industries, among others. Improved understanding of energy dissipation and damage assessment is needed to model interactions between human soft tissues and personnel protective equipment with impacting projectiles. Experiments using cadavers, instrumented dummies, and synthetic biomimetic materials measure and model effects of extreme pressure and velocity on soft tissue. Based on these results, standard tests and surrogate materials have been developed to evaluate and rank protective equipment [Fackler and Malinowski, 1985].

Recent work to better understand how impact forces are transmitted through soft tissue have led to the fabrication of instrumented surrogate torsos composed of modified ballistic gelatin (BG) [Fackler et al., 1984] or modified silicones [Simmonds, 2004]. To an extent, these testing platforms mimic the mechanical response of soft tissue and are often instrumented to gather pressure and velocity data during impact. This data is further utilized to validate finite element models, which help to describe the response of the impact on soft tissue. Often lacking in these efforts is the proper match of the surrogate mechanical properties to soft tissue mechanical properties. A closer pairing of the acoustic and mechanical properties of a well-defined synthetic material to natural tissue can improve the data collected from the surrogates, ultimately improving the ability to model impact damage.

Naturally derived BG has been most widely used as a tissue surrogate to develop a wound profile that provides limited injury analysis [Biermann et al., 2004; Hole, 1980]. For over 40 years, BG has been a standard test medium for evaluating the effects of ballistics and firearms on soft tissue [Abe et al., 1996; Nicholas and Welsch, 2004]. Previous research has shown that the elastic modulus of soft tissue varies from 25 to 300 kPa [Dzieman, 1960], with the modulus of BG being approximately 100 to 150 kPa [Amato et al., 1970; Fackler, 1988]. It is readily available, cheap, and easy to process. However, challenges in using BG as a standard test medium are significant. The mechanical properties, for example, are related to the concentration of water in the gelatin. Ideally, model gels would be tested at 37 °C, normal body temperature, but gelatin only provides usable tissue mimetic properties within a narrow temperature range of 3 to 30 °C, and are commonly used at 10 °C. Naturally derived gelatin can have a variable molecular weight distribution that can lead to inconsistent gelatin properties from batch to batch. Finally, procedural differences exist with regard to gelatin processing and testing [Fackler et al., 1984; Nicholas and Welsch, 2004; Dzieman, 1960; Amato et al., 1970], leading to gelatins of differing mechanical properties. This makes independent testing comparisons difficult.

Any surrogate material selected to mitigate these issues and replace BG should possess a well-defined molecular weight or crosslink density to ensure identical gels from batch to batch. The material should exhibit stable mechanical properties as a function of time and temperature relevant to testing conditions. Finally, the material should mimic natural tissue mechanical properties as closely as possible. Triblock copolymers

Report Documentation Page

Form Approved
OMB No. 0704-0188

1. REPORT DATE	2. REPORT TYPE	3. DATES COVERED
01 NOV 2006	**N/A**	**-**

4. TITLE AND SUBTITLE	5a. CONTRACT NUMBER
Multiscale Mechanical Characterization Of Biomimetic Gels For Army Applications	5b. GRANT NUMBER
	5c. PROGRAM ELEMENT NUMBER
6. AUTHOR(S)	5d. PROJECT NUMBER
	5e. TASK NUMBER
	5f. WORK UNIT NUMBER
7. PERFORMING ORGANIZATION NAME(S) AND ADDRESS(ES) **U. S. Army Research Laboratory, Weapons & Materials Research Directorate Aberdeen Proving Ground, MD, 21005**	8. PERFORMING ORGANIZATION REPORT NUMBER
9. SPONSORING/MONITORING AGENCY NAME(S) AND ADDRESS(ES)	10. SPONSOR/MONITOR'S ACRONYM(S)
	11. SPONSOR/MONITOR'S REPORT NUMBER(S)

12. DISTRIBUTION/AVAILABILITY STATEMENT
Approved for public release, distribution unlimited

13. SUPPLEMENTARY NOTES
See also ADM002075., The original document contains color images.

14. ABSTRACT

15. SUBJECT TERMS

16. SECURITY CLASSIFICATION OF:			17. LIMITATION OF ABSTRACT	18. NUMBER OF PAGES	19a. NAME OF RESPONSIBLE PERSON
a. REPORT	b. ABSTRACT	c. THIS PAGE			
unclassified	**unclassified**	**unclassified**	**UU**	**8**	

possessing an *A-B-A* polymer structure, dissolved in a solvent selective for block *B*, are potential candidates as surrogate materials. The elastic modulus of these gels is primarily determined by the molecular weight of the *B* block (molecular weight between entanglements) and the polymer concentration. By adjusting the concentration of polymer in the gel or the molecular weight of the *B* blocks, the elastic modulus of the gels can be tailored to mimic the elastic modulus of different types of soft tissue.

Techniques such as quasi-static and dynamic compression [Moy et al, 2006], and torsion tests can be used to evaluate the mechanical properties of gels on the macro-scale, and instrumented indentation [Oliver and Pharr, 1992] can be utilized to measure the mechanical properties of these materials at the micro-scale. The size scale of the indenter is adequate for investigating heterogeneity on the order of microns [Johnson, 1985; Sneddon, 1965]. Instrumented indentation has been used previously to characterize quasi-static and dynamic properties of thermoset polymers and elastomers [VanLandingham et al., 2005; White et al., 2005]. In the case of polymeric materials, the tip-sample interaction is of critical importance [VanLandingham et al., 2005] because polymers exhibit strain rate sensitivity and time-dependent mechanical phenomena such as creep and stress relaxation.

The use of instrumented indentation for evaluating tissue surrogates is advantageous because the surface compression loading is similar to that of a blunt impact into soft tissue. Significant challenges exist when conducting measurements on materials with an elastic modulus below 1 MPa using contact diameters below 1 micron. Adhesion between the indenter tip and sample surface affect the governing displacement-based Hertzian contact area approximation used to determine the contact area. This in turn affects the mechanical property calculations.

In this work, the mechanical behavior of a traditional BG is compared to two different physically associating gels. A methodology to conduct surface mechanical property measurements (for modulus less than 1 MPa) using instrumented indentation on soft gel systems is also outlined in this paper. In addition, a comparison is made between mechanical properties obtained from both bulk and surface measurement techniques, to highlight the similarities and differences between the materials at differing length scales and frequency regimes.

1.1 THEORY

The governing equations for determining the modulus of elasticity from compression and torsion tests are readily available in the literature [Gent, 1992]. The modulus values reported in this work are the ratio of the average engineering stress to engineering strain in the elastic regime.

The discussion that proceeds is focused on the contact mechanics required to measure the mechanical properties of gels through instrumented indentation utilizing a cylindrical flat punch in an axisymmetric geometry. The cylindrical punch was chosen because the uncertainty in the contact area is not significant compared to other tip geometries, leading to smaller error in measured mechanical properties.

To convert indentation loading data into a modulus value, a relation from contact mechanics [Johnson 1985] is used;

$$E^* = \frac{P}{2rh}, \tag{1}$$

where E^* is the reduced modulus of the indented material, r is the cylindrical radius of the indenter, and h is the displacement into the surface. The reduced modulus is defined as

$$E^* = \left[\frac{1-\nu^2}{E} + \frac{1-\nu_i^{\,2}}{E_i} \right]^{-1}, \tag{2}$$

where ν and E are the Poisson's ratio and elastic modulus of the indented material, respectively, and the subscript i refers to properties of the indenter. If the indenter tip is taken to be perfectly rigid, and the material is purely isotropic, incompressible, and an elastic response is assumed, the indented material modulus becomes

$$E = \frac{3P}{8rh}. \tag{3}$$

To compare this value with uniaxial storage and loss modulus values for an incompressible elastic solid, the relation

$$E = 3G \tag{6}$$

is used.

For indentation with a flat punch, storage and loss moduli are calculated in the following way. Assuming isotropic, elastic and incompressible contact, storage modulus is a function of the dynamically measured stiffness S (or an instantaneous ratio of load to displacement) and is given by

$$E' = \frac{3S}{8r}. \tag{7}$$

This is essentially identical to Equation (3), except that stiffness is measured dynamically. The loss modulus is a function of the measured damping, C, associated with the contact, the excitation frequency, ω, and is given by

$$E'' = \frac{3\omega C}{8r}. \tag{8}$$

Mechanical properties provide an evaluation of the structural integrity of a material as a function of experimental variables. For a blunt trauma test, it is desirable to develop a measure of a material's ability to dissipate impact energy as a function of both force and rate. The energy per unit volume may be used to describe the energy expended to deform the surface and sub-surface material. When considering indentation with a flat punch, the energy absorbed by the material is the area underneath the load-displacement curve. The total displaced volume is

$$V = \pi r^2 h. \tag{9}$$

The relations in this section are used to compute reported mechanical property values presented in this work.

2. MATERIAL

2.1 Ballistic Gelatin

Ballistic gelatin (BG) samples were made from a 20% mass fraction of 250 bloom type A ordnance gelatin that is dissolved into 40°C ultra-pure filtered water. The bloom form of the gelatin is acquired from Gelita USA Inc. (Sioux, IA). Right cylindrical compression specimens were fabricated by pouring the solution into an open-faced aluminum mold and cooling to ambient conditions prior to refrigeration at about 4°C.

2.2 Physically Associating Gels

Physically associating gels (PAG) were made from two triblock copolymers (Kraton Polymers, Houston, TX) consisting of polystyrene (PS) and polyisoprene (PI). Both triblock copolymers consisted of 80% mass fraction triblock (PS-PI-PS) and 20% mass fraction diblock (PS-PI) composition. One gel contained 15% by mass PS and the other gel contained 30% by mass PS, both used as received and identified as PS-15 and PS-30 for this study, respectively. The polymer was mixed with a white, light mineral oil (Mallinckrodt Chemicals, St. Louis, MO) at a ratio of 20% by volume polymer and 80% by volume mineral oil. The solution was placed in a nitrogen-purged vacuum oven at ~150°C and fully dissolved over a period of about 6 hours, being stirred every hour. The melt was then poured onto a flat surface at room temperature. Similarly with the BG, the PAG were molded into right cylinder compression specimens. Both materials were visually semi-transparent and contained no detectable air bubbles in their final state.

3. EXPERIMENTS

3.1 Macro-Scale

The bulk mechanical properties of the BG, PS-15 and PS-30 were obtained using an Advanced Rheometer 2000 (TA Instruments, New Castle DE) and a servo-hydraulic Instron 1331 mechanical testing frame (Instron Corporation, Norwood, MA). Both apparatus were used to characterize the materials from the quasi-static to intermediate strain rates. For higher strain rates beyond 1000 s^{-1}, the Split Hopkinson Pressure Bar (SHPB) was used [Kolsky 1949].

The compression experiments were performed on the rheometer at room temperature using a 12-mm diameter cylindrical specimens that had a thickness of approximately 3-mm. Tests were displacement controlled at rate of 5, 10, 50, and 100 μm/s, until a total displacement of 500 μm occurred, yielding equivalent strain rates of approximately 0.0017, 0.0033, 0.0167, and 0.3333 s^{-1}, respectively. For these compression experiments, the loading surfaces were well lubricated with mineral oil to ensure a uniaxial stress state and to reduce frictional effects. The diameter of the loading plates was larger than the specimen diameter and polished to a mirror finish to reduce the friction between the specimen and the loading platens.

For the other macro-scale experiments, the more traditional uniaxial compression experiments were conducted at a constant strain rate of 1 s^{-1} on a servo-hydraulic Instron 1331 mechanical testing frame. Both the diameter and length of the compression specimens were 12.7 mm, thus yielding a length to diameter ratio of 1. A computer program was written to command an exponentially decaying reference voltage from a WaveTek signal function generator to the Instron control unit to achieve the constant true strain rate. Similarly, mineral oil was used as a lubricant on the specimen ends to minimize the friction at the compression platens interfaces.

3.1.1 High Rate Experiments

Generally, a conventional SHPB consists of a striker, an incident bar (input), and a transmission bar (output). The working principles of such a setup are well documented [Meyers, 1994; Gray, 2000]. Assuming the specimen undergoes homogenous deformation and the incident and transmission bars are of the same diameter and material, the analysis based on one-dimensional wave theory [Kolsky, 1949] shows that the nominal strain rate, $\dot{\varepsilon}(t)$, in the specimen to be

$$\dot{\varepsilon}(t) = -\frac{2c_\circ}{L}\varepsilon_r(t), \tag{10}$$

where L is the original gage length of the specimen, $\varepsilon_r(t)$ is the time-resolved strain associated with the reflected pulse in the incident bar, and $c_\circ$ is the elastic bar-wave velocity of the bar material. Integration of equation (10) with respect to time gives the time-resolved axial strain of the specimen. The nominal axial stress, σ, in the specimen is determined using the

equation

$$\sigma(t) = \frac{A_t}{A_s} E_t \varepsilon_t(t), \qquad (11)$$

where A_s is the cross-sectional area of the specimen, $\varepsilon_t(t)$ is the time-resolved axial strain in the transmission bar of cross-sectional area, A_t, and Young's modulus, E_t.

However, the ability of the Hopkinson bar apparatus to obtain a considerable stress response for soft materials such as gels is limited due to a high noise to signal ratio in the transmission bar. The generated incident pulse traveling through a low impedance material is reduced by several orders of magnitude in a metal output bar, in comparison to a specimen with a higher sound velocity such as a metal alloy. To overcome this issue, semi-conductor strain gages were used in place of common resistive foil-type strain gages on the input and output bars. The semi-conductor gages have sensitivity 50-75 times greater than that of traditional foil gages. The semi-conductor gages are bonded at the midpoint on the surface of the aluminum input and output bars and the electrical circuitry is completed through a Wheatstone bridge. The magnitude of the semi-conductor gage signal is approximately 50 times greater than that from the resistive strain gages, which barely register any signal. The lengths of the input and output bars were 2.4384 m and 1.2192 m, respectively.

For a SHPB experiment to be valid when testing soft materials, the specimen should be in dynamic stress equilibrium, in addition to achieving a near constant strain rate during the test. These are accomplished by wave-shaping the incident pulse and having the proper specimen gage length. Gel specimens were fabricated with a thickness of 1.45 mm for its gage length and a diameter of 12.7 mm. High-density insulation foam was used as the pulse shaper and placed at the front face of the incident bar where the striker impacts. Without proper pulse-shaping, the rise time for the gel material would not be sufficient for the specimen to reach dynamic stress equilibrium. A 609.6 mm long striker provided the necessary loading pulse for the gel specimens.

The raw data signals reveal a spike at the beginning of the trace for all gelatin tests. Recent work at high rates by Chen et al. on rubber-like gelatin material also showed an initial spike on the stress-strain traces [Chen et al. 2006]. Chen et al. determined that these spikes are an experimental artifact during the initial acceleration of the axial strain and not an intrinsic material response. To eliminate this artifact, they proposed to alter the specimen geometry from a right cylinder to an annular shape ring. Following this recommendation, the specimen geometry of 12.7 mm outside diameter and 5.33 mm inside diameter was used in our experiments.

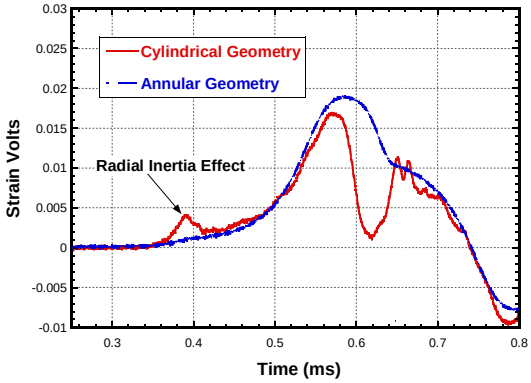

Fig 1. Radial inertial effects of ballistic gelatin.

Figure 1 shows the comparison of the transmitted pulses for ballistic gelatin between an annular ring and cylindrical specimen. This figure shows that the radial inertial effects are eliminated using the annular shaped ring specimen. Using these experimental methods, stress-strain behavior of ballistic gelatin and two PAG gels were obtained at high rates.

3.2 Micro-Scale

PS-15 and PS-30 mechanical properties were measured at the micro-scale using a TriboScope depth-sensing indenter (Hysitron, Inc., Minneapolis, MN) in both quasi-static and dynamic mode. Load and displacement are continuously measured during material loading and unloading at resolutions in the sub-μN and sub-nm range, respectively. For all tests performed in this work, a 250 μm radius flat punch indenter was used. Oscillation frequency varied from 10 to 200 Hz. The material surface was located by manually lowering the tip until an adhesive tensile force was sensed. The indenter was lowered until the load reading became zero. Quasi-static indentation tests at a maximum of 600 nm were carried out at 1, 10, 25, 50, 100, 150, and 200 μN/s controlled loading rates. Unloading rates were approximately the same for each test, and holding times were less than 4 seconds. Data points were collected using active load control, meaning the spring force was subtracted from the measured load in real time to achieve true load rates. Dynamic tests were performed at depths of approximately 500 nm into the sample surface with oscillation amplitudes of about 15 nm. Oscillation frequency varied from 10 to 200 Hz. Indentation data are not reported on BG due to non-repeatability tests since the properties of the BG change so drastically with temperature and relative humidity. The mechanical and geometrical stabilities both were affected by inhomogeneity of the gelatin and evaporation of the water from the surface.

RESULTS AND DISCUSSION

Bulk compression measurements at ~10 ºC indicate BG modulus values of 96 ± 12 kPa at a strain rate of 0.001 s^{-1} and 124 ± 4 kPa at a strain rate of 0.01 s^{-1} to ultimate strains of about 1. The dependence of modulus on strain rate suggests that BG has a significant viscoelastic component to its mechanical behavior.

Dynamic measurements from rheometer experiments confirm this as well. At 0.1 and 10 Hz excitation frequencies, the corresponding loss modulus values were calculated to be approximately 20% of the storage modulus at 10ºC, seen in Figure 2. Storage modulus was about 150 kPa while the loss modulus was about 30 kPa. In theory, the complex modulus (or just "modulus" as it is referred to here) is the vector sum of the storage and loss modulus, which are perpendicular to each other, or about 153 kPa in this case. The modulus measured by compression should be, and is, equal to or less than this value. A major weakness of BG is the sudden decrease of the gelatin structure between 25 to 30ºC over a period of time, making testing at room temperature unreliable.

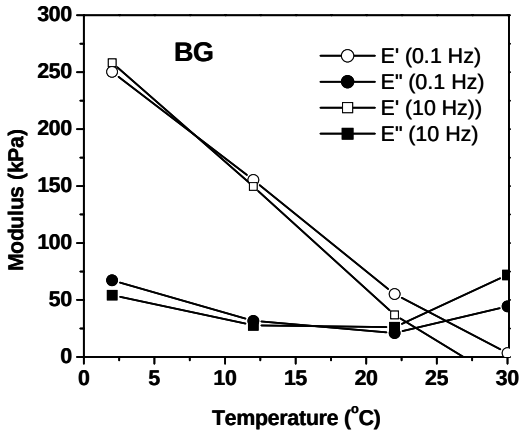

Fig 2. Storage and loss modulus properties for BG as measured dynamically at 0.1 and 10 Hz with the rheometer from 0 to 30 ºC. Properties vary greatly as a function of temperature

Gel compression tests at room temperature for both PS-15 and PS-30 showed virtually no rate dependence in the considered loading range of 5 to 100 µm/s. PS-30 had an average measured modulus value of about 31.5 kPa, while PS-15 averaged to about 30 kPa. For all tests, the average modulus value for PS-15 is lower than that for PS-30; however, for two of the loading rate conditions, the values are within the standard deviation of the measurements. As compared to BG, the synthetic gel modulus values are significantly lower (by a factor of 4 to 5).

Dynamic measurements agree with the compression test data trends at room temperature. The complex modulus values of PS-15 and PS-30 are approximately 18 kPa and 30 kPa, respectively, over a range of 0-50 ºC. It is unclear why such a detectable modulus difference exists using the dynamic method as compared to quasi-static uniaxial compression, although the two techniques agree better for the PS gels than for the BG. This could be due to the fact that the compression samples had lubricated boundaries while the dynamically measured samples did not. Dynamic measurement may also cause a localized heating effect in the sample, inducing a lack of thermal equilibrium in the material. Unlike BG, PS-15 and PS-30 have fairly stable mechanical properties in the range of 0 to 50ºC, which make their properties easier to assess at room temperature compared to BG.

Indentation measurements were conducted to compare micro-scale mechanical properties to those measured at the macro-scale. Quasi-static indentation tests on PS-15 and PS-30 yielded a rate-dependent hardening response that was not seen with the compression tests. For both gels, a higher loading rate yielded a higher load at the same displacement into the surface. An example of this effect is seen in Figure 3. Only the linear portions of the loading curves in Figure 3 were considered for modulus measurements (typically from approximately 100 nm to 600 nm of indentation depth). The non-linear portions of the loading curves are believed to be due to the inertia of the indenter fixture and artifacts from the closed-loop control system, and so are discarded from the analysis.

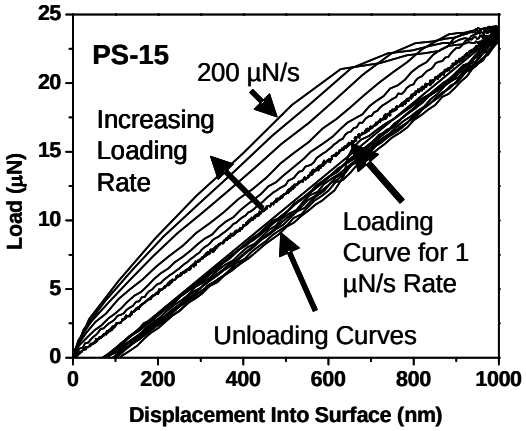

Fig 3. Loading and unloading curves for loading rates of (1, 10, 25, 50, 100, 150 and 200) µN/s on PS-15, illustrating the time-dependent response of the material. Results were similar for PS-30.

Because these measurements are based on Equation 3, the measured modulus represents a vector sum of the storage and loss modulus. The initial and final non-linear portions of the loading curve are likely due to the inability of the closed-loop load control system to track the small forces involved. If the assumptions made are correct, the *P* versus *h* plot should be linear for a flat punch. Therefore, the slope of the line is critical to determining the measured modulus, while the origin of

the fit will not influence the measured modulus and require a fit to both the load and the intercept. This is not the case with other indenter geometries such as spherical, Berkovich, conical, or cube corner.

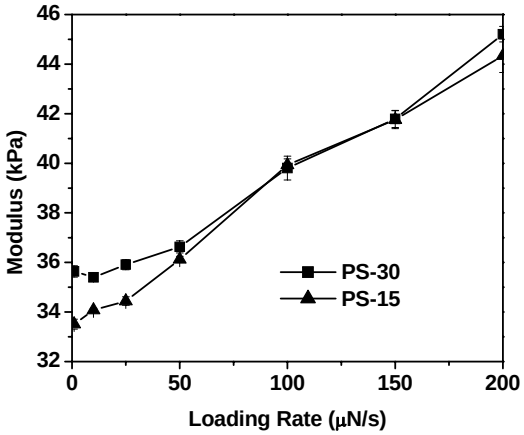

Fig 4. Indentation modulus of PS-15 and PS-30 as a function of loading rate. Error bars represent one standard deviation in the measurements.

Modulus values for PS-15 and PS-30 as a function of loading rate are reported in Figure 4. Interestingly, the modulus of PS-15 is lower than that for PS-30 at loading rates below 50 μN/s and above this rate the modulus values are within the standard deviation of each other (~1 kPa). It is possible that at such high loading rates this behavior is an artifact of the machine's collection capabilities, or it could point to the fact that the mobility for each material becomes similar at higher loading rates. For stress rate comparison, the stress rate during indentation loading at 50 μN/s was similar to the rheometer loading rate of 10 μm/s.

The observed major noticeable difference between the rheometer compression data and the indentation data for PS-15 and PS-30 is the evidence for rate dependence in the materials. Although the average stress in the direction of applied force during indentation is much less than for compression tests, the stress field underneath the flat punch indenter is much different than that for uniaxial compression. For example, at about 85% of the radius value, the stress underneath the tool is twice the stress incurred at the center of the flat punch. Uniaxial compression assumes an evenly distributed stress state in the direction of loading. However, at the edge of the flat punch, stresses are very large (theoretically infinite). Therefore, this highly-stressed annular boundary area, which is not present in bulk compression tests, may contribute to the rate dependence of the two materials.

Likewise, the modulus measured by the indentation technique is also higher than that for the rheometer compression tests. A reason for the higher modulus may be tensile stress buildup that contributes to frictional forces, as the incompressible gel material is stretched across the face of the indenter. The average storage modulus of both PS gels was 47 ± 8 kPa and the loss modulus was 2.4 ± 1.0 kPa when the data was averaged over the frequency range of 10 to 200 Hz, as measured by dynamic indentation. These averages yield complex modulus values only slightly higher than those found using the quasi-static indentation technique, which could be due to heating effects at higher frequencies. However, the measured storage and loss modulus varies quite a bit over the frequency range (Figure 5). At 10 Hz, both materials had a storage modulus of 39 kPa, which is still higher than values determined using the rheometer, but are within close agreement of the quasi-static data. This discrepancy between indentation storage modulus and the rheometer values may be because indentation measurements were dependent on the calibrated dynamic response of the indentation instrument, which has a much greater stiffness than that of the contact. Therefore, the dynamic contact stiffness and damping measurements may not be sufficiently sensitive to properly sense the contact. Similar to the trend with the loss modulus measured via the rheometer, there is a consistent increase in its magnitude as a function of frequency. Time-temperature superposition measurements (not shown) made via the rheometer and shifted to frequencies above 100 Hz show a monotonically increasing modulus compared to the decreasing modulus observed in this range for the dynamic indentation measurements. As measured with indentation, the loss modulus is 0.20 ± 0.03 kPa at 10 Hz and 3.7 ± 0.1 kPa at 200 Hz for both PS-15 and PS-30. The loss modulus was 0.5 % of the storage modulus at 10 Hz and 16 % at 200 Hz.

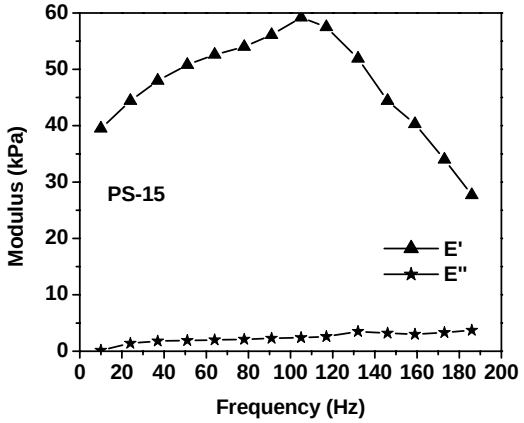

Fig 5. Storage and loss modulus of PS-15 as measured dynamically with the flat punch indenter over a range of 10-200 Hz. Results for PS-30 were similar.

Figures **6**(a) and **6**(b) show the typical macroscopic stress-strain response obtained for the gels under uniaxial compression at 1/s and ~2500/s strain rates, respectively. All the data from different specimens are within the shown error bars. At the intermediate rate of 1/s, the

flow stress of the ballistic gelatin is significantly higher than that obtained for the other two PAGs. In addition, the ballistic gelatin has a linear behavior up to about a strain of 1, the maximum strain of the intermediate strain rate experiments. On the other hand, stress-strain response of both PS-15 and PS-30 is non-linear and starts to reach a maximum stress. The ballistic gelatin and PAGs regain their original shape upon unloading even when the specimens are strained to 1, showing a non-linear elastic behavior.

In contrast, the macroscopic stress-strain response at the high rate is quite different from that observed at 1/s for the three materials. As shown in Fig. 6b, the PS-15 gel behaves almost like the ballistic gel, at the high strain rate of ~2500/s. This indicates that the PAG gels are much more rate sensitive, compared to the ballistic gelatin.. As also observed in indentation modulus measurements, measured values of moduli for PS-15 and PS-30 are similar at elevated loading rates under macroscopic measurements (Figure 4).

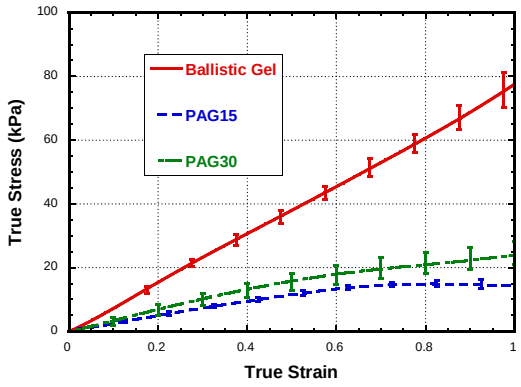

(a)

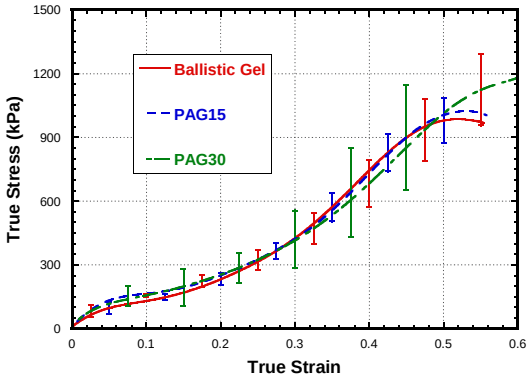

(b)

Fig 6. Summary of the stress-strain response for ballistic gelatin, PS-15 and PS-30 at (a) 1/s and (b) ~2500/s.

Figure 7 shows the flow stress as a function of strain rate at different strains for all materials investigated. PAGs have higher rate sensitivity than the ballistic gelatin, and the difference in the rate sensitivity increases with strain. This is an important observation, which will influence the penetration behavior of these three materials. During penetration, ballistic gelatin and PAG are deformed and fail under high rates. All three materials seem to have an almost identical deformation behavior at high rates. However, ballistic gelatin and PAG deform differently at low rates. It is expected then that they will deform differently away from the penetration-target interaction zone. At this time, we do not understand how that will influence the penetration behavior of the ballistic gelatin and PAG. Only a computer simulation, taking into account the observed constitutive and failure behavior of these materials, could provide an insight to this.

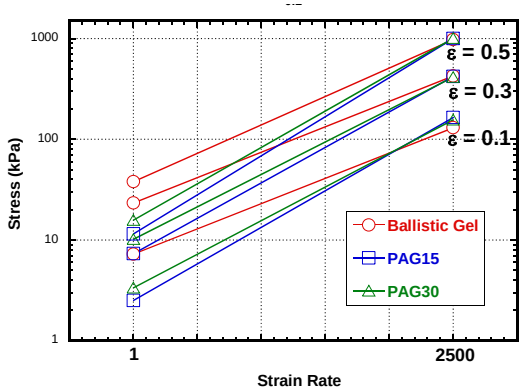

Fig 7. Rate sensitivity of ballistic gelatin, PS-15 and PS-30.

CONCLUSIONS

The modulus of BG was successfully measured using rheometric and compression techniques on the macro-scale. Two physically associating gels, PS-15 and PS-30, based on swollen triblock copolymers, were found to exhibit mechanical properties within the range of BG. Although the modulus values of PS-15 and PS-30 were less than BG, they were still at the lower end of the modulus range reported for soft tissue (~25 kPa). Even though only two specific gels were studied in this work, the gel systems may be tailored to have their modulus increased. Compared to BG, both PS-15 and PS-30 were found to have a greater degree of thermal stability. A successful methodology was developed for mechanically characterizing materials with a modulus below 1 MPa using instrumented indentation, which applies to a number of other soft material systems. Both macro and micro-scale tests of PS-15 and PS-30 yielded similar modulus measurements. Rheometer measurements found little rate dependence on either PS-15 or PS-30, while micro-scale measurements and Hopkinson bar tests revealed rate dependent behavior, and similar trends. Interpretation of the dynamic mechanical properties of the two gels measured with instrumented indentation and comparisons to the loading rate effects were difficult.

More extensive work on these and other similar material systems is planned for the future.

ACKNOWLEDGMENTS

This research was supported in part by TFJ's and AMF's appointment to the Postgraduate Research Participation Program at the U.S. Army Research Laboratory administered by the Oak Ridge Institute for Science and Education. The authors wish to acknowledge our fellow colleagues at ARL for their contribution to this work; Mr. William Edmanson, for his effort in the gelatin preparation and specimen fabrication and Mr. Allan Gunnarson for his assistance in the testing and data reduction.

‡ Certain commercial equipment and materials are identified in this paper in order to specify adequately the experimental procedure. In no case does such identification imply recommendations by the Army Research Lab nor does it imply that the material or equipment identified is necessarily the best available for this purpose.

REFERENCES

Abe, H., Hayashi, K. and Sato, M. (Eds.), 1996: Data Book on Mechanical Properties of Living Cells, Tissues, and Organs, Springer-Verlag, Tokyo.

Amato, J.J., Billy, L.J., Gruber, R.P., Lawson, N.S., and Rich, N.M., 1970: Vascular injuries: An experimental study of high and low velocity missile wounds. *Archives of Surgery* **101**, 167-174.

Biermann, P.J., Ward, E.M., Cain, R.P., Carkhuff, B., Merkle, A.C., and Roberts, J.C., May 2004: Development of a Physical Human Surrogate Torso Model (HSTM) for Ballistic Impact and Blast. In Proceedings of the 36th International SAMPE Technical Conference, Long Beach, CA.

Chen, W., Ge, Y., Song, B., and Weerasooriya, T., 2006: Characterization of Extra-Soft Materials under Dynamic Compression. To be submitted to the *Journal of Mechanics and Physics of Solids*.

Drzal, P.L. and Shull, K.R., 2003: Origins of Mechanical Strength and Elasticity in Thermally Reversible Acrylic Triblock Copolymer Gels. *Macromolecules*, **36**, 2000-2008.

Dzieman, A.J., 1960: *A provisional casualty criteria for fragments and projectiles*, Edgewood Arsenal Maryland Report #2391.

Fackler, M.L., Surinchak, J.S., Malinowski, J.A., and Bowen, R.E., 1984: Bullet Fragmentation: A Major Cause of Tissue Disruption. *J. of Trauma-Injury Infection & Critical Care*, **24**, 35-39.

Fackler, M.L. and Malinowski, J.A., 1985: The Wound Profile: a Visual Method for Quantifying Gunshot Wound Components. *J. of Trauma-Injury Infection & Critical Care*, **25**, 522-529.

Fackler, M.L., 1988: Wound ballistics: A target for error. *International Defense Review*, **8**, 895-897.

Gent, A.N., 1992: *Engineering with Rubber: How to Design Rubber Components*, Hanser Publishers, New York.

Gray, G. T., 2000: Classical Split Hopkinson Pressure Bar Testing: In Mechanical Testing and Evaluation. American Society for Metals, Metals Handbook, **8**, 462-476.

Hole, L.G., 1980: Anatomical Models Based on Gelatin and the Influence of Garments on Impact Damage. Shoe & Allied Trade Research Association, Satra House.

Johnson, K. L., 1985: *Contact Mechanics*. Cambridge University Press, New York.

Kolsky, H., 1949: An Investigation of the Mechanical Properties of Materials at Very High Rates of Loading. *Proc. of the Royal Society of London*, **B**, **62**, 676-700.

Meyers, M.A., 1994: *Dynamic Behavior of Materials*. John Wiley and Sons, New York.

Moy, P., Weerasooriya, T., Juliano, T. F. and Vanlandingham, M. R., 2006: Dynamic Response of an Alternative Tissue Simulant, Physically Associating Gels (PAG), Proc. Of the 2006 SEM Annual Conference on Experimental Mechanics, June 2006, St. Louis, Missouri.

Nicholas, N.C. and Welsch, J.R., 2004: *Ballistic Gelatin*, Institute for Non-Lethal Defense Technologies Report, Penn State Applied Research Laboratory.

Oliver, W.C. and Pharr, G.M., 1992: An Improved Technique for Determining Hardness and Elastic Modulus Using Load and Displacement Sensing Indentation Experiments, *J. Mater. Res.*, **7**, 1564.

Sato, T., Watanabe, H., Osaki, K., 2000: Thermo-Reversible Physical Gelation of Block Copolymers in a Selective Solvent. *Macromolecules*, **33**, 1686-1691.

Simmonds, K.E., Matic, P., Chase, M., and Leung, A., 2004: www.nrl.navy.mil, 2004 NRL Review.

Sneddon, I.N., 1965: The relation between load and penetration in the axisymmetric Boussinesq problem for a punch of arbitrary profile. *Int. J. Engng Sci.* **3**, 47-57.

VanLandingham, M.R., Chang, N.K., Drzal, P.L, White, C.C., and Chang, S.H., 2005: Viscoelastic characterization of polymers using instrumented indentation I. Quasi-static testing. *J. of Poly. Sci. Part B: Poly. Phys.* **43** 1794-1811.

VanLandingham, M.R., Juliano, T.F., and Hagon, M.J. 2005: Measuring tip shape for instrumented indentation using atomic force microscopy. *Meas. Sci. and Tech.* **16**, 2173-2185.

White, C.C., VanLandingham, M.R., Drzal, P.L., Chang, N.K. and Chang, S.H., 2005: Viscoelastic characterization of polymers using instrumented indentation II. Dynamic testing. *J. Poly. Sci. B Poly. Phys.*, **43** 1812-1824.